LAWRENCE
LIVERMORE
NATIONAL
LABORATORY

LLNL-TR-463081

Primer on Use of Multi-Spectral and Infra Red Imaging for On-Site Inspections

J. R. Henderson

November 24, 2010

Disclaimer

This work performed under the auspices of the U.S. Department of Energy by Lawrence Livermore National Laboratory under Contract DE-AC52-07NA27344.

Primer on use of Multi-Spectral and Infra Red Imaging for On-Site Inspections
John Henderson
October 2010

1.0 Introduction

The purpose of an On-Site Inspection (OSI) is to determine whether a nuclear explosion has occurred in violation of the Comprehensive Nuclear Test Ban Treaty (CTBT), and to gather information which might assist in identifying the violator (CTBT, Article IV, Paragraph 35) Multi-Spectral and Infra Red Imaging (MSIR) is allowed by the treaty to detect observables which might help reduce the search area and thus expedite an OSI and make it more effective. MSIR is permitted from airborne measurements, and at and below the surface to search for anomalies and artifacts (CTBT, Protocol, Part II, Paragraph 69b). The three broad types of anomalies and artifacts MSIR is expected to be capable of observing are surface disturbances (disturbed earth, plant stress or anomalous surface materials), human artifacts (man-made roads, buildings and features), and thermal anomalies.

The purpose of this Primer is to provide technical information on MSIR relevant to its use for OSI. It is expected that this information may be used for general background information, to inform decisions about the selection and testing of MSIR equipment, to develop operational guidance for MSIR use during an OSI, and to support the development of a training program for OSI Inspectors. References are provided so readers can pursue a topic in more detail than the summary information provided here.

The following chapters will provide more information on how MSIR can support an OSI (Section 2), a short summary what Multi-Spectral Imaging and Infra Red Imaging is (Section 3), guidance from the CTBT regarding the use of MSIR (Section 4), and a description of several nuclear explosion scenarios (Section 5) and consequent observables (Section 6). The remaining sections focus on practical aspects of using MSIR for an OSI, such as specification and selection of MSIR equipment, operational considerations for deployment of MISR equipment from an aircraft, and the conduct of field exercises to mature MSIR for an OSI. Finally, an appendix provides detail describing the magnitude and spatial extent of the surface shock expected from an underground nuclear explosion.

2.0 Objective for use of MSIR

If there is a seismic event or other data to suggest there has been a nuclear explosion in violation of the CTBT, an OSI may be conducted to determine whether a nuclear explosion has occurred and to gather information which may be useful in identifying the party responsible for conducting the explosion. The OSI must be conducted in the area where the event that triggered

the inspection request occurred, and the inspected area must not exceed 1,000 square kilometers, or be more than 50 km on aside (CTBT Protocol, Part II, Paragraphs 2 and 3). One of the guiding principles for an inspection is that it be effective, minimally intrusive, timely, and cost-effective [Hawkins, Feb 1998]. In that context, MSIR is one of several technologies that can be used during an aircraft overflight to identify ground regions of high interest in a timely and cost-effective manner. This allows for an optimized inspection on the ground.

The primary purpose for MSIR is to identify artifacts and anomalies that might be associated with a nuclear explosion, and to use the location of those artifacts and anomalies to reduce the search area that must be inspected from the ground.

The MSIR measurements can have additional utility. The multi-spectral measurements of the ground can be used for terrain classification, which can aid in geological characterization of the Inspected Area. In conditions of where light smoke or haze is present, long-wave infrared imaging can provide better imaging of the ground than is possible with standard visible imagery.

3.0 MSI and IR Fundamentals

3.1 MSI and IR Properties

The simple demonstration of using a prism to separate white light, from the sun or an incandescent light bulb, into its component colors is familiar to most people. The technical term used to describe the color of light is its wavelength. Humans can see light with wavelengths from 0.4 microns (a micron is one millionth of a meter), which is purple, to 0.7 microns, which is red. Light with shorter wavelengths is called ultra-violet, and with longer wavelengths, infrared. The infrared can be further characterized as the near infrared (0.7 to 1.0 microns), short-wave infrared (1.0 to 2.5 microns), mid-wave infrared (3.0 to 5.0 microns), and the long-wave infrared (7.5 to 13. 5 microns).

Different objects have different apparent colors because they reflect light differently. Leaves appear green because they reflect that color more strongly than the other colors in the white light from the sun or another illumination source. Multi-spectral imaging is similar to how a human eye works, except that instead of having 3 different color receptors in the human eye, a multi-spectral imager would have ten to 100 different color receptors. The ability of humans to distinguish many more colors than the 3 color receptors depends on the fact that intermediate colors stimulate more than one color receptor, and that the relative stimulation of each color receptor is used to determine the apparent color of an object. Similarly, the relative colors in a multi-spectral imager can be used to distinguish different materials. Figure 3-1 shows the reflectivity for several different materials in the visible through short-wave-infrared spectral range. The reflectivity as a function of wavelength for each material is called the reflectance

spectrum of that material and can clearly be used to uniquely identify the different materials in the figure.

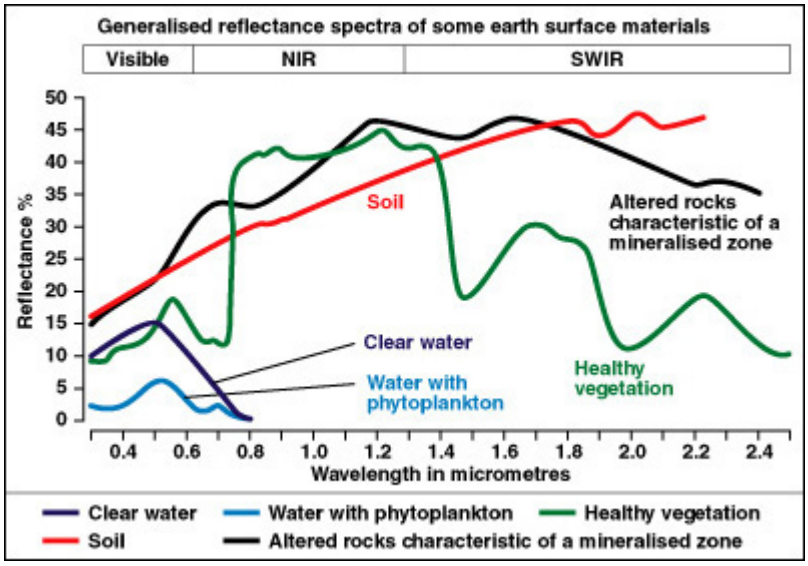

Figure 3-1. Reflectance as a function of wavelength for several materials.

In a real scene, similar materials may have slightly different spectra because of inherent variability in the material, as well as additional factors such as moisture content and amount of weathering. Differences in reflectance spectra are routinely used to assess crop health (using plant stress measurements from Landsat data, for example) and support mineral prospecting.

An interesting property of mid-wave and long-wave infrared is that they are present in greater amounts for warmer objects. One way to observe this is to use a piece of regular glass to block the infrared light from a fireplace fire. It is easy to feel the warmth from the fire on your hand, but putting a piece of glass between your hand and the fire blocks the infrared, and the warmth conveyed by the infrared, but does not block the visible light. The fact that regular glass blocks infrared light will be revisited when we discuss operational aspects of deploying an MSIR sensor. Here the key point is that an infrared imager can detect warmer regions in a scene because of their greater emission of infrared light.

3.2 MSIR Data Analysis Considerations

Thermal and multi-spectral imaging is routinely performed in a commercial/government context, generating standard data products used for agricultural, mineral prospecting, and other resource management purposes. The challenge for MSIR in the OSI context is to identify UNE observables present in a variable spectral and thermal environment, where there may not be any relevant pre-event data to use as a reference for the most sensitive techniques, such as change detection. In this context, the focus will be on anomaly detection (looking for spatial regions

unexpectedly different from adjoining regions) to identify regions for more detailed inspection, and the goal would be to find observables that can narrowly localize the UNE surface ground zero, such as plant stress or the presence of thermal hot spots. The value of the MSIR data is enhanced if the age of the event generating the MSIR observable can be determined relative to that of the seismic event that triggered the inspection request.

4.0 CTBT Text Applicable to MSIR and Operational Impacts

The CTBT references MSIR both explicitly and implicitly.

4.1 Explicit References to the use of MSIR

The paragraphs referred to in this section are located in Part II of the Protocol.

Paragraph 69b explicitly calls out "multi-spectral imaging, including infrared measurements, at and below the surface, and from the air, to search for anomalies or artifacts." By the definition of core equipment in Paragraph 37, MSIR is considered core equipment.

Per Paragraph 70, MSIR can be used in the initial and continuation inspection periods.

The use of MSIR measurements from overflights is governed by Paragraph 79 for the initial overflight, which does NOT call out multi-spectral or infrared measurements and presumably excludes them, and Paragraph 80 for additional overflights, which does explicitly allow MSIR measurements. Additionally, Paragraph 73 specifies that the conduct of additional overflights is subject to the agreement of the inspected State Party (ISP). It thus appears that MSIR measurements from overflights may be made only if the ISP agrees to additional overflights.

As a practical matter, MSIR is expected to have its greatest utility from overflights, with less utility from surface or sub-surface measurements, so the question of whether additional overflights will be allowed during a particular inspection significantly impacts the potential utility of MSIR.

Paragraph 80 imposes the requirement on MSIR equipment used for an additional overflight that it be "portable [and] easily installed" on the aircraft. In the case of infrared equipment, normal aircraft window materials do not transmit the full range of infrared light the equipment might use to function optimally. It may thus be necessary to either (1) install a special infrared window in the aircraft, which presumes the aircraft type is known in advance so the proper size infrared window can be brought with the equipment, (2) use an open window, port or door on the aircraft, or (3) attach the infrared equipment to the outside of the aircraft.

Paragraph 82 states "The inspected State Party shall have the right to provide its own aircraft, **pre-equipped as appropriate in accordance with the technical requirements of the relevant operational manual**, and crew. Otherwise, the aircraft shall be provided or rented by the Technical Secretariat." This implies that any special requirements for infrared measurements, such as an open port, must be called out in the operations manual.

Paragraph 84 specifies that up to four members of the inspection team may be on board the aircraft. Given the types of measurements and equipment these four members might be responsible for (specified in Paragraphs 79 and 80), the MSIR equipment would need to be either extremely easy to operate, slaved to point in the same direction as a video or still camera, or operated autonomously in a fixed pointing mode. In the latter case, one could imagine an infrared video camera taking imagery of the ground below the aircraft throughout its flight pattern, with the possible exception of turning the camera off when passing over sensitive sites.

4.2 Implicit Use of MSIR

Article IV of the Treaty contains several paragraphs that permit the use of unspecified data sources. Paragraph 5 allows the use of national technical means, as consistent with international law, to verify compliance with the Treaty. Paragraph 11 allows the development and use of additional monitoring technologies, including satellite technologies, for verification. Paragraph 37 allows for the use of data from the International Monitoring System or any relevant technical information to be used as the basis for a request for an On-Site Inspection. MSIR from other data sources, such as commercial satellite data, is clearly allowed and may have a role prior to the OSI, such as preparation of information for the inspectors, as well as possibly providing supporting information during the OSI if new and useful satellite data is acquired during the OSI.

5.0 Scenarios

Five general nuclear testing scenarios are described here for completeness: an underground nuclear explosion (UNE), which is the baseline scenario for this primer; a surface test; a test at sea; an atmospheric test; and a test in space. The discussion here will focus on those aspects of each scenario that are relevant to the role of MSIR to reduce the search area to locate and acquire information on the nuclear explosion.

5.1 Underground Nuclear Explosion (UNE)

An underground nuclear explosion may generate a variety of observables, such as post-shot seismic activity, radioactive releases – gases and/or particles, a post-shot cavity, ground-water displacement, surface evidence (disturbed earth, plant stress), and man-made artifacts (metallic cables, cable spools, tailing piles) [Marshall, 1997]. Most notable of these are formation of a

crater, and a variety of surface effects, such as spallation, from the shock wave of the explosion reaching the surface. A good reference on potential observables for a UNE is Zucca et al., Jan 1995. The phenomenology and observables relevant to MSIR from a UNE are described in Section 6.

5.1.1 Baseline Scenario – 1 kt UNE, 200m DOB

The baseline scenario for this primer is an underground nuclear explosion (UNE) of one kt yield. This was chosen because a UNE seems the most likely nuclear testing scenario, based on nuclear tests conducted in the last 20 years, and that this is the scenario for which MSIR can probably provide the greatest benefit for locating the triggering event. The nominal detection threshold of the International Monitoring System (IMS) is one kt, so this is the nominal minimum yield for which MSIR observables should be considered. In fact, the IMS is likely able to detect explosive events below 1 kt in many regions, and a nominal UNE could be in the 1 to 10 kt range, so 1 kt represents a central evaluation point. Where appropriate, scaling of observables with UNE yield will be discussed.

The depth of burial (DOB) for a contained UNE is typically calculated as DOB ~ 120 m * $Y^{1/3}$, where Y is the yield in kt, Olsen 1993; Adushkin and Leith, 2001; U.S. OTA, 1989]. The 120 m term may vary with rock type and moisture. However, at low yields, containment of radioactive release is more problematic, and a more conservative DOB of 183 to 200 m is recommended [Olsen, 1993]. Here we use 200 m as the DOB. By the scaling relation above, a 10 kt UNE would have a minimum DOB of 260 m.

The baseline scenario applies to either a borehole shot or a tunnel shot, where the DOB is measured from the surface to the location of the explosion.

5.1.2 Deeply Buried UNE

The magnitude of the surface shock scales approximately at the depth of burial to the negative third power (see Appendix A, Section A.2). Increasing the depth of burial quickly reduces the magnitude of the surface shock, so the most likely observables will be those associated with human activities preparing for and conducting the test. This was described in the first OSI Workshop as follows: "In the case of a deeply buried clandestine test the geological and environmental effects may be very difficult to detect and therefore the emphasis should be placed on the identification of cultural features and artifacts." [Russian Federation, 1997]

5.2 Above Ground Test

An above ground nuclear test would cause obvious visible features and radioactive contamination that would make location of ground zero relatively easy. Visual observation is

highly likely to identify GZ, although MSIR might provide confirmation that the blast region is anomalous compared to surrounding surface material. Road traffic and man-made artifacts (cables, instrument shelters, etc) are detectable with MSIR and might help locate GZ.

5.3 Maritime Test

For a maritime test there will likely be floating debris. A combination of visual observation and MSIR would be able to find the debris. For a deep underwater explosion, the energy from the explosion is coupled to the water, and a thermal observable is associated with the debris field, which is expected to be about 1 km in diameter after 24 hours, and up to 10 km in diameter after a week. Thermal imagery would likely be able to locate the debris field for a period of up to several days after the explosion. [Zucca et al., Jan 1995] An airborne thermal camera might be the most effective means to locate the surface debris field, and would be capable of either day or night observations.

A nuclear explosion near the surface of the water will produce a surface debris field, but is not expected to generate much of a thermal observable because the energy of the explosion is not well-coupled to the water.

5.4 Atmospheric Test

Sensors in the International Monitoring System are dedicated to locating and characterizing an atmospheric nuclear test. GPS and DSP satellites have sensors dedicated to the detection of atmospheric nuclear tests and would be able to confirm the nuclear nature of the explosion and its location. MSIR could be used to track the path of debris on the ground to assist in the acquisition of samples.

5.5 Space Test

GPS and DSP satellites have sensors dedicated to the detection of exo-atmospheric nuclear tests and would be able to confirm the nuclear nature of the explosion. MSIR is not expected to be relevant to a nuclear test in space.

6.0 Phenomenology and Observables

The five broad categories of MSIR observables used here are:
(1) Disturbed earth
(2) Plant stress
(3) Human artifacts
(4) Thermal effects, and
(5) Anomalous materials

We have chosen these categories because they have the clearest linkage to the MSIR instrument specification and operational requirements. In fact, the same underlying phenomena may generate observables in several categories, such as the surface shock creating disturbed earth and plant stress. Also, some observables might be considered as members of several categories (e.g., recent traffic on dirt roads might be considered disturbed earth or a human artifact).

The first priority in the use of MSIR is to reduce the search area by identifying regions of potential interest. Once the site of the event has been located, OSI measurements are performed to determine whether the event that triggered the OSI was a nuclear explosion or not. In this context, there might be value in having MSIR measurements of other events such as an earthquake, a chemical explosion, or a mine collapse in order to distinguish comparable observables for those events from a nuclear explosion. Briefly, an earthquake may be distinguished from a UNE because the spatial extent of the surface disturbances will be much greater and oriented along the fault line. A chemical explosion of sufficient size and depth of burial might be hard to distinguish from a UNE (hence the value of the Non-Proliferation Experiment, see Section 8.1) because it would have similar surface shock and human artifact observables. However, chemical explosions of that magnitude used in mining are typically surface or near-surface explosions that are detonated in ripple fire mode, resulting in much less surface shock than a UNE would generate, and surface observables consistent with mining activities. A mine collapse would likely have a different seismic signal than a nuclear explosion and is unlikely to generate surface shocks comparable to the baseline UNE, hence should be readily distinguished from a UNE.

Table 6-1 summarizes some of the MSIR observables, sorted by the size of their spatial footprint. The Table also provides additional information on the observables that would be useful in specifying an MSIR instrument for an OSI. The observables are described in more detail in the following sections. Note that these sections assume favorable weather conditions. Since MSIR measurements probe surface characteristics of the ground, rain, snow, and wind-borne dust may alter the spectral characteristics of the observables and should be taken into account when interpreting the MSIR data.

It is important to keep in mind that these observables are not equally likely to be present at a given UNE. This is discussed further in Section 12 in the context of equipment specification but is summarized here to provide some context when reviewing the observables in detail. Human artifacts will be present at any test and are hard to succinctly characterize because their specific characteristics will likely depend on the location and organization conducting the UNE. Disturbed earth and plant stress depend on sufficient surface shock so may not be present at all UNE's of interest, and the plant stress observables may have faded by the time the OSI is conducted. Thermal effects have not been demonstrated at time scales relevant to an OSI, so

there is little information available to evaluate the likelihood of their presence. Anomalous materials have been measured with local sampling, but it is unknown what spatial resolution and spectral bands are needed to reliably detect them with MSIR and it seems likely that some level of containment failure is needed, which means that a radiation survey is probably a more effective detection technology.

Observable	Phenomena	Spectral Region	Spectral Resolution	Spatial Resolution	Temporal Behavior
Air and Satellite Accessible (> 10 m spatial resolution)					
Vegetative stress	Surface shock	VNIR (0.4-1.1 um) SWIR (1.3 & 1.45 um)	Low (≤100 nm)	10-30 m goal ≤ 1 km req'd	peak at 48-56 hours, low after 7 days, senescence - weeks
Surface disruption - spectral	Surface shock	VIS, NIR, SWIR req'd LWIR useful	Low to Med	10-30 m goal ≤ 1 km req'd	weeks if dry, hours to days if rain/wind likely
Surface "fluffing" - thermal mass	Surface shock and spall	Thermal IR (LWIR)	None	10-30 m goal ≤ 1 km req'd	Need to take data around maximum ΔT (e.g. local noon-2 pm)
Presence of geochemical gases	Surface fracture from shock	LWIR and ???	High	<=20 m goal 100 m req'd	Week to ~ 1year
Thermal hot spot	Heat convection through fractured material	Thermal IR (LWIR)	None	1 m goal < 10 m req'd	TBD to form Stable for years
Air Accessible, Satellite Access Marginal (~ 1 m spatial resolution)					
Thermal plume	Hot gas or liquid at or near surface	Thermal IR (LWIR)	None	0.3 m goal ≤ 10 m required	Highly variable (days to weeks?)
Material plumes	Sub-surface material migration with hot gases/liquids	VIS, NIR, SWIR req'd LWIR useful	Low to Med	0.3 m goal ≤ 10 m required	Permanent until covered with local dirt/debris
Air/Ground Accessible Only (< 1 m spatial resolution)					
Spectral &/or thermal artifacts compared to nearby vegetation and geology	Man-made artifacts	All	Low to Med	0.1 to 0.3 m goal ≤ 1.0 m required	weeks to months
Road-like thermal anomalies	Surface disruption from recent traffic	Thermal IR (LWIR)	None	0.1 to 0.3 m goal ≤ 1.0 m required	Days to weeks, Best signature around maximum Δ^T

Table 6-1. Summary of some of the MSIR observables of a UNE. The table is organized by the spatial size of the observable. The spectral region, spectral resolution, and spatial resolution are noted for the purpose of specifying an MSIR instrument. Note that satellites with 0.5 m spatial resolution and multi-spectral capability are becoming commercially available as of 2010, so there is some satellite accessibility to the observables with the finest spatial features.

6.1 Disturbed Earth Observables

Disturbed earth observables can be due to the surface shock or other geological phenomena such as collapse of the explosion cavity propagating to the surface and appearing as a subsidence crater. In either case, the result is that sub-surface material is exposed on the surface, either through mixing with surface material, because it has been thrown over surface material, or because cracks or fissures have opened up. The spectral properties of the sub-surface material can be different than those of the surface material because (1) the materials are different, (2) weathering changes the spectral properties of the ground materials, (3) the moisture content is different, or (4) the surface texture changes. (A simple example of surface texture affecting spectral properties is that a region with significant surface cracks will be darker at all visible wavelengths than a smooth region of the same material.) The main method of detecting disturbed earth regions is to compile spectral data for the Inspected Area, identify regions with comparable spectral properties, and then select out those regions that are small in spatial extent and spectrally different from the other regions.

Many of these observables would be detectable by visual observation, and would also be detectable by MSIR. One value of MSIR is that it has the potential to differentiate between recent events and old events because of their spectral differences. This could be important if a nuclear test is conducted in a region where there are pre-existing craters. There is good synergy between MSIR and other inspection techniques.

It is important to note that the geological disturbed earth observables have spatial sizes on the surface of a few 10's of meters or less [Hawkins and Wohletz, 1996; Adushkin and Spivak, 1994] and the surface shock observables have characteristic sizes of 200 meters or more (see Section 6.1.1).

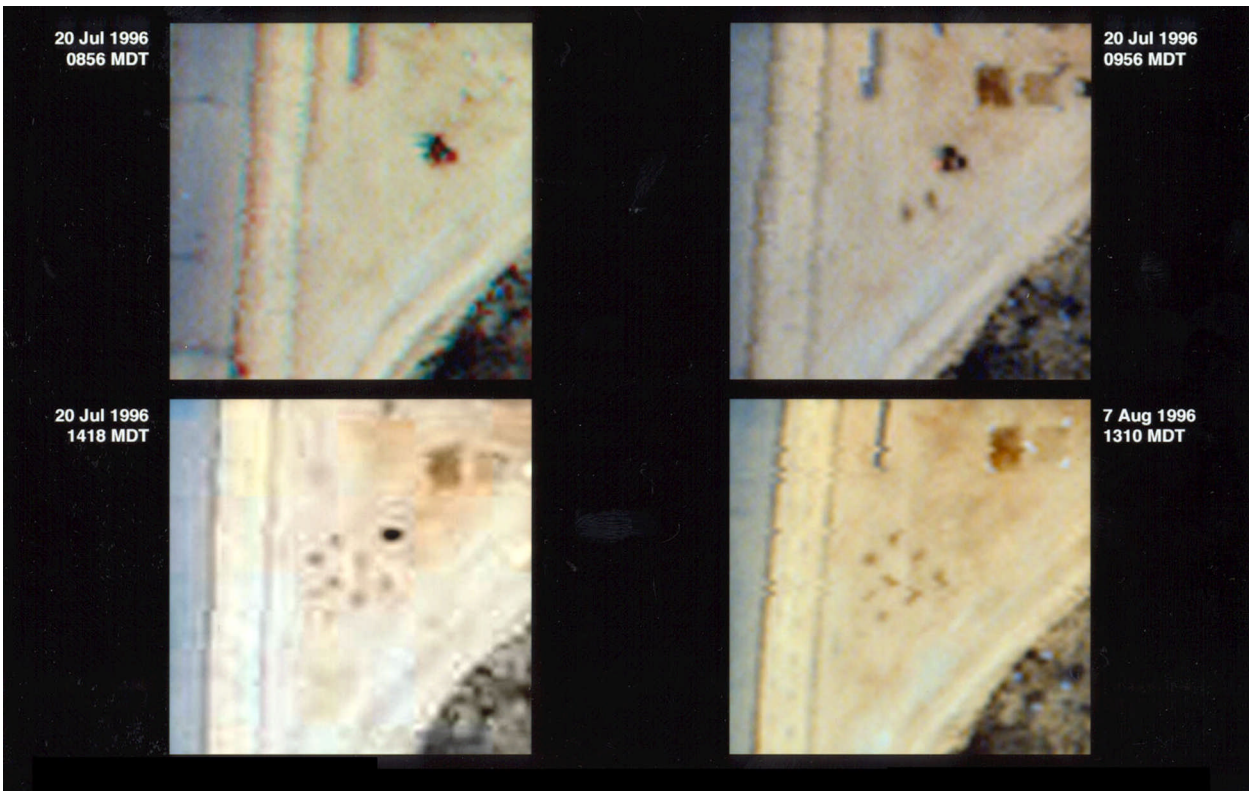

Figure 6.1-1. False color images taken with MSI including the near IR showing the persistence and observability of disturbed earth. The upper left image was taken before any activities. The upper right image shows the results after two holes have been dug and filled in. The lower left image shows the results for six holes dug and filled. The lower right image shows the same scene after 18 days.

6.1.1 Magnitude and Spatial Extent of Surface Shock

Some of the disturbed earth observables and the plant stress observables are due to the effects of the shock wave from the nuclear explosion reaching the surface. Consequently, the magnitude and spatial extent of those observables depends on the magnitude and spatial extent of the surface shock.

The magnitude, direction and spatial extent of surface acceleration is reviewed in detail in Appendix A. The magnitude of the surface acceleration and its spatial footprint will depend on the UNE depth of burial, the yield of the UNE, the coupling of the energy from the UNE to ground material, and the local geology. Surface acceleration has been measured for a number of previous UNE's and is adequately characterized for the purpose of developing MSIR observables. In general, the spatial footprint of surface motion will have a characteristic size of approximately the DOB, although local geology may introduce significant deviations from the circularly symmetric pattern one would expect for homogeneous geology.

The peak acceleration at the surface can be approximated by

$$a^* Y^{1/3} = A * (R/Y^{1/3})^{-3}$$

where the acceleration a is in g's, Y is the UNE yield in kt, A is a coefficient that depends on the ground material, and R is the slant range from the UNE to the surface point in meters. For the nominal scenario of 1 kt yield with a DOB of 200 m, the acceleration at SGZ can vary from 1.0 g's to 67 g's depending on the ground material. Empirical relations for the surface acceleration for different ground materials are provided in Appendix A, section A.2.

It is important to note that the surface acceleration will be approximately radially directed away from the explosion point, so the surface acceleration will be primarily vertical near SGZ, approximately 45 degrees from normal at distances from SGZ equal to the DOB, and primarily horizontal beyond that. This may be important for how surface material is thrown by the ground motion, or for the impacts to vegetation, such as shearing of branches. For comparison, earthquakes typically have primarily horizontal surface motion [Anderson and Brune, 2006], so the extent to which surface effects can be attributed to horizontal or vertical motion can help to localize SGZ as well as discriminate a UNE from an earthquake. However, local geology can significantly modify these simple expectations, as can be seen in the surface acceleration shown for the NPE in Figure A-3.

6.1.2 Acceleration Crater

For an underground explosion with a very shallow depth of burial, surface materials may be accelerated to the point that they are ejected away from surface ground zero (SGZ), leaving a surface crater and probably ejecta trails leading away from SGZ. This would be apparent visually, and would probably leave spectral observables due to the different material exposed on the surface.

6.1.3 Collapse Sink

The cavity formed after the explosion generally collapses, resulting in a rubble chimney propagating upward from the cavity to the surface. If this rubble chimney reaches the surface, a visible subsidence crater will form. This would be apparent visually, and would probably leave spectral observables due to the disrupted material exposed on the surface. The size of this feature is somewhat larger than the cavity, and would be a few 10's of meters in size for explosions in the 1 to 10 kt range.

6.1.4 Depression

If there is downward motion of the surface due to cavity collapse, but the rubble chimney does not reach the surface, a depression crater will form. The amount of surface disruption will be much less than for a collapse sink, and MSIR observables would be possible from either the surface acceleration from the explosion or from the later slumping of surface material. The size of this feature is somewhat larger than the cavity, and would be a few 10's of meters in size for explosions in the 1 to 10 kt range.

6.1.5 Shock-wave features

The shock wave from the explosion can result in additional impacts. These include cracks, fractures, pressure ridges (linear ridges of disturbed surface material), ground disturbances (overturned earth due to lofting of the surface), faults (linear cracks in the surface with horizontal or vertical offsets between the sides), rock falls (on nearby high-slope areas), and ground slump (downslope movement of surface material). These features will all generate surface spectral changes of varying magnitude with a spatial footprint comparable to the depth of burial for the features centered around SGZ, and with spatial sizes dependent on the local topology for rock falls and ground slumping.

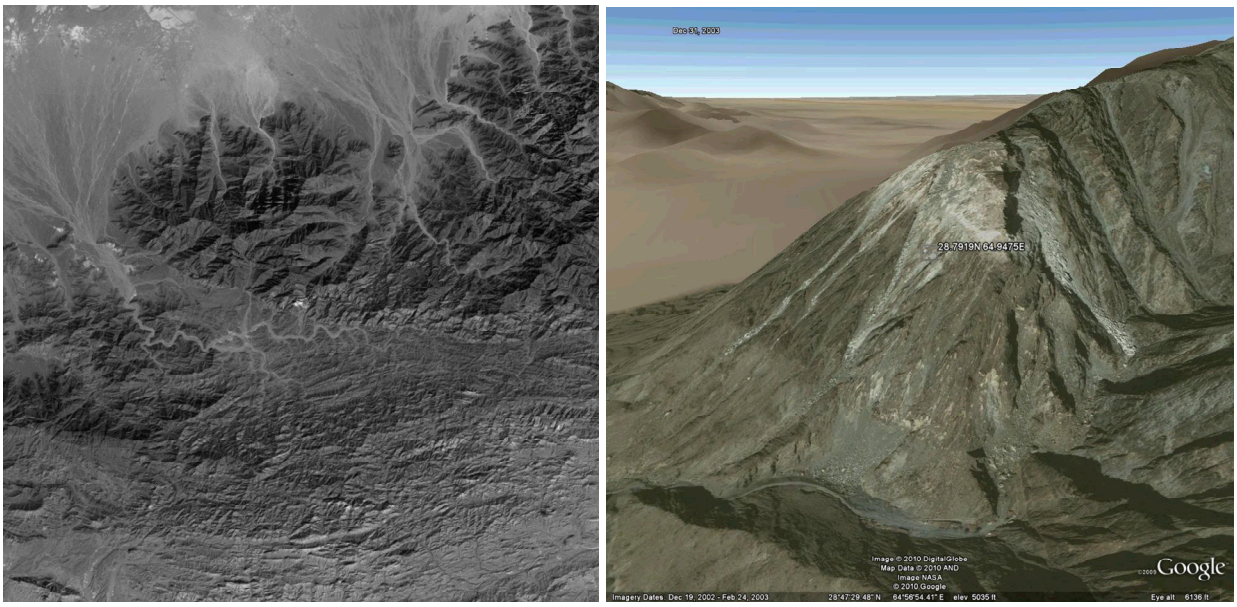

Figure 6.1-2. Disturbed earth imagery after the 28 May 1998 Pakistani underground nuclear test. Left: Landsat blue band data for a 30 km x 30 km (1000 pixel X 1000 pixel) region centered on the suspect UNE location (white spot in center). The data is from 29 June 1998, one month after the event. Right: Imagery of that location from 2003, with apparent rock slides down the slopes.

6.1.6 Other geological features

The pressure from the shock wave as well as local heating can impact underground water behavior with resultant changes in the water table level (detectable in wells) and water body levels (such as ponds or lakes). Visual inspection could detect these changes and might be more readily performed than MSIR, but if the altered water behavior increases the moisture content of the surface, those changes might be detectable with MSIR but not necessarily visible. The spatial footprint of altered surface moisture content will depend on the local geology.

In cases where the water body level does not change, agitation from the ground motion may change the water turbidity, and comparison of water turbidity between local water bodies by visible and MSIR observations may serve to help localize the ground disturbance.

6.2 Plant Stress

Spectral changes due to plant stress have been demonstrated for a variety of plant stressors [Carter, 1993; Carter, 1994]. Aerial measurements were made after the NPE [Pickles, December 1995], and plant stress was observed from spectral measurements (specifically using the ratio of reflectance at 690 nm to that at 420 nm) for all vegetation in surface regions that experienced 0.2 g or greater. The spatial resolution for these measurements was 0.7 m. The amount of plant stress measured was correlated with the surface acceleration for that location. The amount of plant stress peaked 56 hours after the explosion, and relaxed to approximate pre-NPE levels 7 days after the explosion. Early oak leaf senescence (leaf death typically seen as the change to fall leaf colors), was observed in the regions near surface ground zero by observers on the ground post-NPE.

Subsequent measurements of individual plants [Pickles and Carter, 1996] showed that the amount of plant stress increased with drops of 1, 2, or 3 feet, which was estimated to be the amount of surface motion in regions that showed plant stress during the NPE. Note that this corresponds to the second peak of acceleration described in Appendix A, which is typically the largest acceleration at the surface.

Many groups currently use multi-spectral techniques to measure specific plant stressors, perform plant species identification, and terrain categorization, amongst other uses for multi-spectral data. This literature is well-covered in the Applied Journal of Remote Sensing, the International Journal of Remote Sensing, and other journals. A key observation from a review of this literature is that different groups have developed different optimized indices for the effect they are seeking to measure, and that these indices likely depend on the specific plant, season, stressor, spectral resolution and bandpass of the detection system, and spatial resolution of the sensor. The implication is that current relevant indices, such as the Normalized Differential

Vegetation Index (NDVI), Carter's plant stress index (R965/R420 or R695/R760) [Carter, 1994], and the modified Normalized Differential Water Index (NDWI) [Wang et al., 2009], are probably a good starting point for developing a plant stress indicator for a UNE, but that data from the NPE, nuclear tests, earthquakes, and chemical explosions will need to be used to develop a generalized optimum indicator of plant stress for OSI's. It is also important to note that different plants vary in their response to a given stressor. Ideally, the spatial resolution of an MSIR sensor would be 0.5 m or finer to resolve individual plants [Pickles, 2010]. Figure 6.2-1 gives illustrative spectra for healthy and stressed plants as well as soil. Since the soil spectrum is similar to that of stressed plants, the spatial resolution must be sufficient to distinguish these two, lest the soil spectrum cause the vegetation spectrum to look stressed.

Note that plant stress may also result from thermal affects (see Section 6.4), altered water (surface and sub-surface) flow (see Sections 6.1.6 and 6.4.2), or radiation exposure (see Section 6.5). In the extreme case, trees and shrubs have been observed to be killed by the ground motion along tectonic faults (visible as surface fractures) and rock slides from megaton UNEs [Rhoads, 1976].

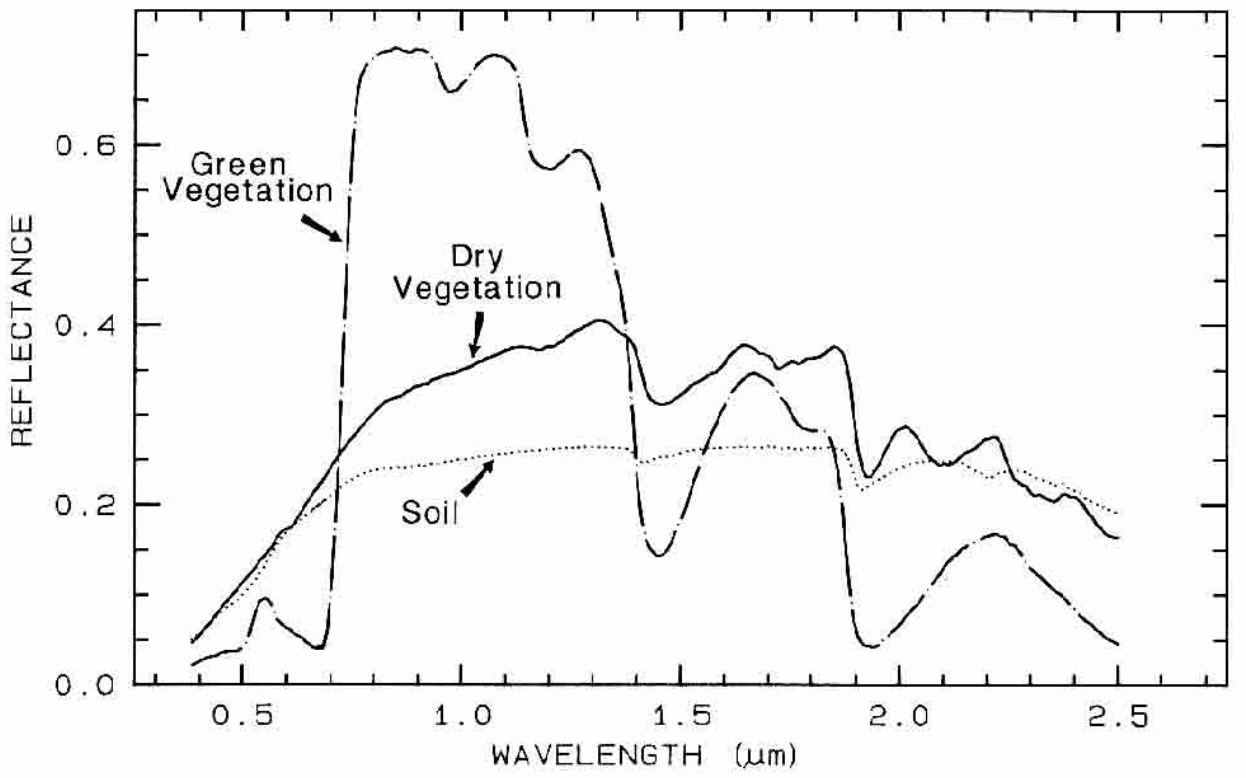

Figure 6.2-1. Comparison of spectra for healthy (green) and stressed (dry) vegetation. Note that healthy vegetation has a dip in reflectance around 0.69 um, and that soil is spectrally similar to dry vegetation.

6.3 Human Artifacts

There is a wide range of human artifacts that can be detected with MSIR as well as visually. The value of MSIR in supplementing visual observation is that it can provide additional information. For example, MSIR imagery of dirt or gravel roads can show whether they have been used recently, even where that is not apparent under visual observation. Similarly, a tailings pile with fresh material on it can likely be discriminated from an old tailing pile because the fresh material will not be weathered and will be spectrally distinct from the weathered tailings.

Roads (paved, dirt and gravel), buildings, vehicles, man-made materials (especially metals), cables, cable spools, moved earth, debris piles, and recent road traffic on dirt or gravel roads all are likely to have spectral features that distinguish them from their surroundings. One advantage of MSIR is that there are analysis algorithms that can automatically identify these spectrally anomalous regions from the surrounding material. Figure 6.1-1 shows an example where MSIR imagery readily highlights disturbed earth where there has been digging. Recent vehicle traffic on dirt and gravel roads typically generates readily detected spectral changes by disturbing the road surface.

6.4 Surface Thermal Effects

There are four phenomena that might cause thermal anomalies to appear on the ground surface following a UNE. First is heat from the explosion propagating to the surface by thermal conduction. Second is a plume of hot water or steam that is generated from underground water flow intersecting hot rock near the explosion cavity (heat convection). Third is heating on the surface from the venting of hot gases from the explosion. Fourth is thermal anomalies due to lofting of the surface material. Note that these four observables can have very different spatial extents, and that they may induce plant stress observables as well as thermal observables.

6.4.1 Conducted Thermal Footprint

A one kiloton explosion deposits 4.2×10^{12} Joules of energy into the surrounding ground. Here we assume that all of that energy is deposited as heat, but a significant portion of that energy goes into fracturing and moving surrounding material. The heat capacity of typical ground materials is 0.2 cal/gm-C or larger with high moisture content, and the density is typically in the range of 2 to 3 gm/cc. Assuming a 200 m depth of burial and that a sphere of 200 m radius is uniformly heated by this energy, the average temperature rise of this mass of ground is 0.06 C. Allowing for a more typical partition of the explosion energy between thermal and kinetic effects, and accounting for the thermal gradient, the temperature rise on the surface would be 0.01 C or less. Typical thermal fluctuations in a scene are approximately 1 C, so this small a

temperature rise would not be detectable. The eventual thermal footprint would have a width comparable to the depth of burial.

Further, the time for a heat pulse to propagate a given distance R scales as $R^2/(4\alpha)$, where α is the thermal diffusivity. For R=200 m and a typical rock thermal diffusivity of 1.3×10^{-6} m^2/sec, the time constant is of order 10^{10} sec, or over 200 years. Thermal conductance will not provide a measurable signal either in amplitude or on a time scale relevant to an OSI.

A useful reference for more detailed calculations and measurements of energy deposition and transport for a UNE is Johnson et al., 1959.

6.4.2 Thermal Plumes

Underground water flow may intercept the hot region near the explosion and either be heated or turned to steam. If this water or steam migrates to the surface, either because the underground flow has been disrupted or rock fracture has opened a low resistance path to the surface, there will be a hot spot at the surface. The spatial extent of this hot spot will depend on the flow rate and size of the path of flow. The timing of when the hot spot appears, the amount of temperature rise, and the duration of the hot spot will depend on the amount of sub-surface water flow and the temperature where the flow intersects the hot explosion region. The hot spot would probably be of order one meter in size. For a sufficiently fractured region around the hot zone, a circulation cell of air might be established which would convect heat to the surface.

Two papers have described temperature rises of up to 8C on the surface in the vicinity of UNE's [Sakharov, 1998; Busygin et al., 2000]. The second paper describes measurements made 2 to 25 years after the UNE. The description of thermal arcs several 10's of meters in length is consistent with convection from a fractured zone surrounding the hot zone of the explosion. The thermal footprint over a borehole UNE had a width of 50 m or larger. The thermal measurements were made from an aircraft. Clearly these thermal plumes can persist for a long period of time. The question for an OSI is how long does it take for the thermal plume to be generated after the UNE?

Underground water flow that is not redirected may still generate detectable thermal changes. If the water flows past the hot zone and continues to where it feeds a surface body of water, that body of water will heat up over time. Monitoring the temperature of local water bodies and investigating any with unusually high temperature may help localize a UNE.

6.4.3 Venting of Hot Gases

Hot gases from the explosion itself may be vented to the surface if containment fails. The venting would be relatively short on the time scale of an OSI, but if there was sufficient heating of the surface material, a hot spot might persist for a few days. Radiation detection is probably a more effective way to identify the location of surface venting from containment failure.

6.4.4 Surface Thermal Mass Anomalies

A less obvious phenomena is that the thermal mass of the surface changes when it has been shocked. If the surface material is either compacted because of settling from the shock, or "fluffed" by being lofted from a vertical surface shock, the density and thermal conductivity of the surface material might be significantly changed. During the course of a day, these regions may show thermal differences because they will respond differently to solar heating. For example, a region that has been fluffed will have lower density and less thermal conductivity. This means that it will heat up faster when the sun is shining on it. If the MSIR overflight is timed properly to observe the ground when these thermal heating differences are maximized (probably around noon on a cloud-free day), regions of altered surface properties might be identified. The standard way to make measurements of the thermal properties of surface materials is to make thermal image measurements throughout the day. This allows calculation of the thermal properties (thermal conductivity and heat capacity) of the materials, which might distinguish between shocked and undisturbed surface materials. The practical difficulty of this method for an OSI is that it would require multiple flights with the MSIR equipment throughout a day, and it is not clear the Inspected State Party would permit that many flights or whether the these measurements would provide enough value to justify that much time from the inspectors. The size of such a region would be comparable to the depth of burial, and the effect would be strongest near the center.

6.5 Material Migration and Containment Failure

There are two phenomena that might result in anomalous materials on the surface. If there is containment failure, materials from the UNE can be deposited on the surface at the location of venting and downwind from that location. The UNE materials might be detectable directly, or might chemically react with surface materials and be detected as anomalous that way [Dubasov, 1998].

The second phenomena is where volatile materials are brought up from the sub-surface through heat-induced migration. For thermal flows as described in section 6.4.2, volatile sub-surface materials, such as Iodine or Arsenic, might be entrained in the hot flow of water, steam, or air,

and carried to the surface where they would precipitate or evaporate out [Hall et al., 1997; Button, 1998; Button and Hall, 1998].

There is a third phenomena in this category, the presence of geological gases on the surface, but the concentration of these gases would be too low to be detectable with MSIR. The idea is that fracturing of the rock around a UNE allows more of the geological gases to escape to the surface. Also, heating of certain rock types might generate CO_2. In both cases, the gas concentrations are not high enough for detection by an airborne MSIR instrument. [Olsen, 1993]

7.0 Use for Geological Characterization

Satellite and aircraft spectral measurements are routinely used to perform ground classification – identifying ground regions of similar rock or vegetation types by their spectral similarity. Spectral measurements could be used for an OSI in the same way, permitting a limited number of inspections of ground sites (particularly for rock/mineral types) to be extrapolated to a larger area. This information could be acquired from satellite data prior to entry of the inspectors, or from airborne MSIR data acquired on an additional overflight and analyzed as part of the OSI. The concern with acquiring this data as part of the OSI is that the Inspected State Party may not agree to an additional overflight, in which case there might be no MSIR measurements, and that adding the task of analyzing MSIR data for geological information will further burden already-busy inspectors.

8.0 Analysis of Historical Events and Data

Analysis of previous nuclear tests may provide useful information to better characterize MSIR observables of UNE's. Also, there may be non-nuclear events which can be used to characterize similar observables for the purposes of obtaining information to specify MSIR equipment for an OSI, to develop the MSIR CONOPS for an OSI, and to train inspectors. It is useful to have a list of historical events to review for relevant data, and a list of events that might be used in place of a UNE to mature the use of MSIR for an OSI. The information here is intended to identify events that might be used to mature the use of MSIR for an OSI.

8.1 NTS Nuclear Tests and the Non-Proliferation Experiment

The Non-Proliferation Experiment (NPE) was an underground chemical explosion with a approximate energy of 1.1 kt emplaced 389 m beneath the surface of Rainier Mesa at the Nevada Test Site (NTS). It was executed as a surrogate for a nuclear explosion to test and develop non-proliferation technologies [Kamm and Bos, 1995; Proceedings, 1994].

Table 8.1-1 provides a list of nuclear tests with properties comparable to the NPE [Patton, 1994], suggesting they might be appropriate nuclear tests for MSIR measurements. There are two practical difficulties with using NTS data. First is that no contemporaneous MSIR data was taken during these events. The most relevant MSIR data would be that from the Thematic Mapper (TM) on the Landsat 5 satellite. Since this satellite was launched in 1984 and is still operational, it provides a valuable potential source of information to compare MSIR observables for UNE's over the last 25 years. The Thematic Mapper performs spectral imaging in multiple visible and infrared bands with 30 meter spatial resolution, and thermal infrared measurements with 120 meter resolution.

The second practical difficulty with using historical data is that years of weathering, erosion or deposition of material, and possible site remediation mean the surface MSIR observables are likely to have been significantly altered from what would be observed during a timely OSI. This means there would be little value in collecting current MSIR data on these historical tests.

Event	DOB (m)	$m_b(P_n)$	Date	Time	Lat (N)	Long (W)
NPE	390	4.16	22Sep93	07:01	37.20	116.21
Hunter's Trophy	400	4.18	18Sep92	17:00	37.21	116.21
Mineral Quarry	389	4.51	25Jul90	15:00	37.21	116.21
Misty Echo	384	4.79	10Dec88	20:30	37.20	116.21
Harzer	637	5.62	06Jun81	18:00	37.30	116.33
Kearsage	616	5.64	17Aug88	17:00	37.30	116.31

Table 8.1-1. Comparison of some parameters for the Non-Proliferation Experiment (NPE) chemical explosion and several nuclear tests at the NTS. DOB is the Depth of Burial, m_b represents the seismic amplitude of the test, and Lat(N) and Long(W) are the latitude and longitude of the events.

8.3 1998 Nuclear Tests

There are four suspected nuclear tests that were conducted in 1998. India conducted tests on May 11 and May 13. Pakistan conducted tests on May 28 and May 30. These tests have the same limitations as the Nevada Test Site tests, which is that the best source of commercially available data is probably the Thematic Mapper on Landsat 5.

8.4 North Korean Nuclear Tests

North Korea conducted suspected nuclear tests on 9 October 2006 and 23 May 2009. These tests are very relevant to the OSI problem and the maturation of MSIR because International Monitoring System data is available, and because commercial MSIR satellite data is available with better spatial resolution or better spectral resolution (but typically not both) than Landsat Thematic Mapper data.

8.5 Chemical Tests

Some mining companies routinely detonate kiloton quantities of explosives, but the conditions under which those detonations occur have some important differences from a UNE. There are three factors which might cause the observables from a large mining explosion to deviate from the observables from a comparably sized UNE. First is that the explosives are ripple-fired (i.e., detonated as a series of smaller charges rather than the entire charge instantaneously). This means that the surface accelerations and ground disturbances are smaller but for a longer time than for a UNE. Second, the explosions are either surface blasts or deep mine blasts, either of which will cause the spatial extent and magnitude of surface shock to deviate from that of a UNE. Third, areas of mining tend to be in continuous use, which means that disturbed earth and plant stress observables are more likely to be due to the accumulation of weeks of explosions rather than the most recent explosion. It is unclear whether surface accelerations reach the 0.2 g needed for plant stress or the higher levels probably needed for disturbed earth observables.

8.6 Earthquakes

Earthquakes might generate several of the features possibly associated with a UNE – disturbed earth and ground fissures are likely, and plant stress is a possibility depending on the amount of surface shock and ground movement. The difficulty with basing field measurements on an earthquake is that one cannot predict the location or timing of the earthquake. This means that one would need to have arrangements made to fly an MSIR system to the site of the earthquake to take the desired data within one to two weeks of the earthquake (shorter if one is interested in measuring plant stess). Recently, a team from Rochester Institute of Technology made MSIR measurements on the earthquake in Haiti [see http://www.wired.com/wiredscience/2010/01/haiti-3d-flyover/]. That example might be taken as a template for how to have resources in place to take relevant earthquake data when possible.

There is a qualitative difference between most earthquakes and a UNE, which is that the ground motion for an earthquake is typically horizontal, whereas the shock from a UNE is primarily vertical in the region near ground zero where the shock will be strongest [Anderson and Brune, 2006].

9.0 Open Issues with Regard to Utility and Equipment Specification

9.1 Platform for MSIR measurements

The CTBT describes MSIR measurements being made during an Additional Overflight, if one is permitted by the Inspected State Party. MSIR measurements are also allowed from the ground, and below the ground. Ground measurements might be useful if one can get the MSIR

instrument to a location where there is a good view of the surrounding terrain. This would permit MSIR measurements in addition to the airborne measurements or instead of them if an additional overflight is not allowed. Below-ground measurements might be useful if one is looking for spectral anomalies or using the spectral information to do geological characterization. In both of those cases, the main benefit of surveying a large area to look for anomalies has been lost, and there are typically more efficient means to obtain the same information.

If the Inspected State Party (ISP) is cooperative with the OSI, several options may be of interest for the MSIR measurements. Unmanned Aerial Vehicles (UAV's) can provide aerial coverage of the Inspected Area, and a member of the ISP could potentially control the UAV flight path to ensure no restricted areas were observed. This might permit MSIR measurements throughout the day (see Section 6.4.4), and would potentially decouple the MSIR measurements from the logistics concerns of Additional Overflights. MSIR systems have been designed and deployed that are UAV-compatible. Another option is to use a tethered balloon to loft the MSIR equipment to a height where it can survey the surrounding region. Both the UAV and tethered balloon deployments potentially require significant increases in the amount of equipment the Inspection Team must bring with them, as well as additional training of Inspectors to use that equipment.

Satellite data might be used to search for many of the MSIR observables, the main limitation being the spatial resolution required to look for some of the human artifact observables. As commercial satellites have better spatial resolution and more capable spectral imaging sensors, satellite data becomes more relevant to OSI needs. Satellite data is clearly allowed in the treaty as part of the information used to prepare the inspectors before entering the Inspected Area. It would be useful to be able to provide the Inspectors with additional data after entry if relevant satellite data is collected during the OSI. For example, the Landsat satellite passes over a given area every 16 days, so it is conceivable there may be several Landsat data sets available during the course of an OSI. One of the characteristics of shocked ground is that it weathers and settles more rapidly than surrounding regions, so its changing spectral nature can be used to identify that region of interest for more detailed inspection. A sequence of Landsat images from before the triggering event and continuing through the OSI might be able to provide this information and identify a region for inspection that might otherwise not have been detected.

9.2 Development of MSIR Equipment Specification

There are several areas where there is currently insufficient information to generate a detailed specification for the MSIR equipment. First, the MSIR observables have not been sufficiently well-characterized to fully specify the spectral channels and spatial resolution needed to confidently detect them. Second, the likelihood of detecting a specific observable has not been

determined, although satellite data might be analyzed on recent UNE's to improve this situation. Third, the role of MSIR in the inspection process (survey the entire Inspected Area, or perform a detailed look at regions of interest) is currently unclear. Fourth, the concept of operations for MSIR measurements during an OSI has not been detailed. These shortcomings will be addressed in some of the following sections, but clearly analysis of satellite data and field experiments to collect and analyze airborne MSIR data are needed to improve the situation.

There is an additional feedback loop for the equipment specification which includes the results of data analysis. The development, testing, and maturation of MSIR data analysis algorithms is a substantial topic by itself, but it is worth commenting here that it will take some time to leverage the analytical expertise built in other areas (e.g., airborne MSIR for mineral prospecting) to the OSI problem. It is possible that the results of maturing the analysis algorithms will be requirements that would result in MSIR equipment more capable of detecting the desired observables.

10.0 Potential use of Satellite data

Three uses of MSIR satellite data have been identified. First is the use of satellite data on historical and more recent UNE's to determine if certain observables are present at a UNE, and to characterize those observables. Preliminary work analyzing satellite data has shown that disturbed earth and human artifact observables are present and appear useful to reducing the search area [Henderson et al., 2010].

The second use of MSIR satellite data is to identify regions of interest to prepare the inspection team before entry into the Inspected Area. The third use of MSIR satellite data is to use pre-event satellite data, post-event satellite data, and any airborne MSIR data from the OSI to perform change detection and additional data analyses that might be more sensitive than analyzing any one of these data sets in isolation.

11.0 MSIR Measurement CONOPS

The concept of operations (CONOPS) for making the MSIR measurements depends on why those measurements are being made, and how they are made. Both topics should be resolved further and appropriate information included in the Standard Operating Procedure for MSIR.

11.1 Purpose of MSIR Measurements

While the purpose of MSIR measurements to reduce the search area is clear, the timing and detailed purpose for MSIR measurements may vary depending on the specific conditions of a given OSI. When there is little initial information available, MSIR measurements could have

significant value in surveying the entire Inspection Area (IA) and identifying regions of interest for detailed inspection. There are two related consequences of this scenario. First, that these measurements must be made as soon as possible to provide information to guide ground inspection activities, and second, that these measurements must be made before there is any significant ground activity that might mask human activity observables, such as road traffic, that might indicate regions of interest. In this case, it is expected that the Inspection Team Lead would plan for a rapid Additional Overflight so the MSIR measurements could be made as soon as possible. In this case, the MSIR equipment must be compatible with a wide area search of the entire IA.

If regions of interest are identified prior to the Additional Overflight, the role of MSIR may be more to characterize those regions for use in prioritizing the detailed inspection from the ground. For example, if there is information suggesting that the UNE was conducted in a tunnel complex with a known entrance, but more detailed information on the location of surface ground zero (SGZ, directly above the UNE) would be valuable for deploying seismic sensors, MSIR measurements might be used to look for disturbed earth or plant stress observables that would indicate SGZ. Another example is where MSIR measurements are desirable over inaccessible terrain for the purpose of characterizing the geology to interpret seismic data. For these examples, there is much less urgency in the timing of the MSIR measurements, and the MSIR equipment do not need to be capable of wide area search.

11.2 MSIR Deployment Options

There are at least five options for how MSIR equipment might be used in support of an OSI:

(1) Use portable equipment on local aircraft for additional overflights
(2) Use UAV controlled locally with ISP observer monitoring flight path and observations
(3) Contract aircraft with dedicated MSIR equipment to conduct flyover from accessible airfield, potentially with ISP observer on board
(4) Use balloon to loft equipment (options range from low-altitude tethered to high altitude drifting/controlled)
(5) Use satellite data

Option 1 is clearly within the language of the treaty, but there are certain practical aspects that must be considered. First is that typical aircraft window materials do not transmit thermal infrared (8 to 12 microns) light, and that plexiglass, the most common aircraft window material, may not transmit light beyond 1.1 microns. (Lexan and glass are the other two common aircraft window materials and transmit light from the visible to 3.2 and 2.6 microns respectively.) If the MSIR equipment includes a thermal imager, that instrument either needs to have a special optical window, be mounted in an open port or window of the aircraft, or be mounted external to the aircraft, such as on the landing gear of a helicopter. Even for visible viewing, access to a

suitable view is important. Lessons learned from the October 1997 US Table Top Exercise [Gough, 1998] include that the utility of overflights depend on the size, transparency and location of windows or viewing ports. This consideration has impact on the selection of the aircraft and the mounting requirements for the MSIR equipment.

Use of a UAV (option 2) might avoid the problem of needing a suitable viewing port if the UAV and the MSIR equipment are chosen to be compatible. The UAV might be flown out of a relatively nearby airport, but not necessarily from within the IA. This would reduce the burden on the limited number of inspectors, since the collection of the MSIR data would be tasked to staff outside the group of inspectors. This option has been discussed since the first OSI Workshop [Zucca, 1997], but there is no consensus on whether this would be in accord with the treaty.

The MSIR measurements might be contracted out to a third party commercial organization (option 3). This would allow equipment selection for either the broad area search or the detailed MSIR inspection of previously identified regions of interest. A further advantage of this option, and potentially option 2, is that there is no need to have an extensive MSIR training program for inspectors since this service would be contracted out. An open issue for both options 2 and 3 is where the data is analyzed and what information is then passed to the inspectors. One option is to have trained experts at the Technical Secretariat.

Using a balloon to loft the equipment (option 4) might be valuable for a limited set of regions of interest, but is probably not suitable to search the entire IA since practical balloon altitudes are a few hundred meters and balloons would require many redeployments to cover the entire IA.

The use of satellite data (option 5) has been described in Section 10. It should be considered as a backup option in case the ISP does not allow an additional overflight. The notional scenario is that the PTS would acquire and analyze satellite MSIR data, and provide the results to the inspection team. The results would need to include the type of observable, its central location, and its spatial extent to ensure the inspection team had all relevant information to put the MSIR information in the correct context with other information.

12.0 Equipment Requirement Considerations

Table 6-1 showed that the spatial resolution, spectral region and desired spectral resolution varied with the particular MSIR observable under consideration. The challenge is to develop a set of MSIR instrument requirements that balance the practical need for the equipment to be easy to handle and operate with the technical finding that more information enhances the sensitivity to MSIR observables.

The CTBT requires that the equipment be portable and easily installed [CTBT Protocol, Part II, Paragraph 80] and there is an operational need to minimize the amount of inspector effort to operate the equipment and analyze the data. Both of these requirements push the MSIR equipment specification to a minimal set of instruments that would be easy to use, such as an imaging spectrometer that covers the visible and near infrared regions (0.4 to 1.0 microns) and a thermal infrared camera. The user interface for MSIR instrument control and data storage must be easy to use.

As technology has developed, the trend in remote sensing is to use more spectral regions (e.g., visible, near-infrared, etc.) and more spectral bands in each region (higher spectral resolution). This greater amount of information allows the detection and separation of increasingly subtle distinctions in surface materials. Also, the trend has been toward higher spatial resolution, which allows finer features to be distinguished, which means their spectral properties are not washed out by averaging with other features and that materials can be distinguished better. This was demonstrated when the ability of two sets of satellite data to detect human artifacts associated with a UNE were compared [Henderson et al., 2010]. GeoEye-1 data with 4 spectral bands and 3 meter resolution was able to detect roads and mining activities proximate to the 2009 North Korean test, whereas the same analysis algorithm applied to Landsat Thematic Mapper data with 6 spectral bands and 30 meter spatial resolution was not able to identify that area as anomalous compared to the surrounding region. Despite fewer spectral channels, the higher spatial resolution of the GeoEye-1 data allowed the unique spectral features of the observables to be detected. Equipment with more spectral channels and higher spatial resolution will generally be larger and more complex to operate, and will certainly generate more data to analyze which will take more inspector time to review.

A third consideration for the equipment specification is the limit of what equipment is or might be available. There are many reasons to start with an assessment of commercially available equipment to determine if some combination of that equipment would provide an acceptable solution. Commercial equipment generally beats custom equipment when considered against cost, delivery time, availability of spare parts, existence of training materials, demonstrated performance, lack of export controls, known calibration requirements and known performance stability over time. There is often the option of renting commercial equipment to perform field tests, which would likely be a cost-effective way to refine the equipment specification and concept of operations. Some related goals for the equipment were called out in OSI Workshop 2 [Davies, 1998; Brand, 1998]. They are:

- Readily transported from storage area to inspection area
- Little or no re-engineering to be used in aerial platform
- Simple to operate
- Useful for OSI purposes
- Preferably COTS

- Preferably no R&D required
- No installation required
- No interface with aircraft avionics

A fourth consideration for the equipment specification is which observables are most likely to be present, so the equipment specification ensures a capability to detect those. Human artifacts will be present at any test. Disturbed earth and plant stress depend on sufficient surface shock so may not be present at all UNE's of interest. Additionally, any plant stress observables will have largely faded one to two weeks after the event and are unlikely to be present by the time of an additional overflight. Thermal anomalies have not been observed for a UNE at times relevant for an OSI (the existing thermal anomaly measurements were made two or more years after the UNE). Finally, the presence of anomalous materials has been demonstrated with local sampling, but it is unknown what spatial resolution and spectral bands are needed to reliably detect them with MSIR and it seems likely that some level of containment failure is needed, which means that a radiation survey is probably a more effective detection technology.

Finally, one must consider that commercial satellite data is available and how that impacts the OSI MSIR equipment selection and operations. Clearly the OSI data from an additional overflight will be timely and can be taken from overhead or side-looking as preferred. The airborne data should have 0.5 to 2 meter spatial resolution to ensure reasonable sensitivity to human artifacts. A likely scenario is that satellite data will be used to generate a preliminary map of regions of interest. The Additional Overflight would be expected to fly those regions for more detailed inspection and characterization. It would be valuable for the OSI MSIR equipment to have spectral bands corresponding to the satellite data both to confirm regions as anomalous, as well as being able to perform change detection possibly using pre-event satellite data as a reference.

The spatial resolution needs to be considered in more detail because there are important trades. A spectral imager typically has a limited number of pixels across the instrument field of view, and only looks at a slit image of the ground, the second dimension of the detector array being used for spectral information. (Another option is several two-dimensional imagers with spectral filters.) The motion of the aircraft is then used to "pushbroom" the slit across the scene and develop a full spectral image of the scene. The limited number of pixels across the slit means that higher spatial resolution is traded for a more narrow field of view of the ground. If it is intended to make MSIR measurements of the entire Inspected Area (IA), then larger pixels on the ground are necessary to minimize the number of flight passes necessary to cover the IA. If it is intended to use the MSIR measurements to further characterize regions of interest identified from satellite data and the initial overflight, higher spatial resolution is more valuable.

A secondary consideration on the swath width of the MSIR equipment is that pixels at the edge of the swath will be larger than those at nadir (directly below the aircraft), and that there will likely be some spectral artifacts in edge pixels compared to central ones because the illumination angle is different and many surfaces have an angle-dependent reflectivity. These considerations are more important for MSIR equipment used in search mode where the swath width must be as wide as practical. These concerns can be mitigated by flying the aircraft at a higher altitude, but that will likely have a negative impact on other measurements being performed.

While we have focused on using thermal imaging to look for hot (or cold) spots on the ground, multi-band thermal imaging should have utility to look for disturbed earth, and would therefore have utility to detect traffic on dirt and gravel roads. It is an open question whether a multi-band thermal imager or a multi-spectral visible/near-infrared imager will be more sensitive at detecting and characterizing (amount and age) road traffic.

The platform the MSIR equipment is deployed from (see Section 11) will affect the mounting requirements. The Operating Procedure which determines the mounting requirements may also place requirements on the aircraft if the MSIR equipment is to be used from inside the aircraft and view the ground through and open door or window, or if a helicopter is used and the MSIR equipment is mounted to the landing gear. Additionally, the platform chosen will impose size, weight and power requirements on the MSIR equipment.

The likely path to developing a nominal MSIR instrument specification is then to survey the equipment available, identify a visible/near-infrared instrument and a thermal imager that have relevant characteristics, conduct field experiments with those instruments (either purchased, rented, or contracted) to benchmark performance, and refine the instrument specification and concept of operations based on lessons learned and analysis of the experimental data.

Appendix A: Calculation of Magnitude and Spatial Extent of Ground Acceleration

Whether acceleration of the surface will generate a measurable observable depends on the amplitude of that acceleration. The spatial extent (footprint) of that surface acceleration is an important factor in determining how the effects (plant stress and/or surface spectral changes here) of that acceleration might be measured.

The magnitude of the surface acceleration and its spatial footprint will depend on the UNE depth of burial, the yield of the UNE, the coupling of the energy from the UNE to ground material, and the local geology. Surface acceleration has been measured for a number of previous UNE's and is adequately characterized for the purpose of developing MSIR observables.

A.1 Physics of surface motion

The physics of the surface motion has been well described elsewhere [Eisler and Chilton, 1964; Bernreuter et al., 1969]. The compression wave from the UNE travels to the surface, creating an upward acceleration. Where that upward acceleration exceeds the tensile strength of the near-surface material, there is separation of the near-surface material and spalling occurs. Spalling, if it occurs, will be most severe near surface ground zero (SGZ). The initial acceleration is typically a few g's. Once that acceleration is over, the surface layer is in free-fall and experiences an acceleration of -1 g. When it hits the underlying ground layer, called "slap-down" of the surface layer, there is an even greater though shorter upward acceleration which is typically a few to 10's times greater than the initial acceleration. There are subsequent surface accelerations due to reflected stress in the surface layer, but those are typically less than the slap-down acceleration. See Figure A-1 for an illustration of the vertical acceleration over time near GSZ.

Near SGZ, the acceleration is primarily vertical. As one moves out from SGZ, there are radial accelerations and possibly tangential accelerations depending on the inhomogeneity of the underlying geology. Outside of the spall zone, the first acceleration will be the largest. As one continues further from GSZ, reflected waves, shear waves, surface waves and geological anomalies play an increasing role in determining the amplitude and direction of the surface acceleration. Here we confine our analysis to an estimate of the peak acceleration at GSZ, and the characteristics spatial extent of that acceleration. The reader is referred to reference Bernreuter et al., 1969, and references 2 and 3 therein for more detail on ground motion far out from GSZ.

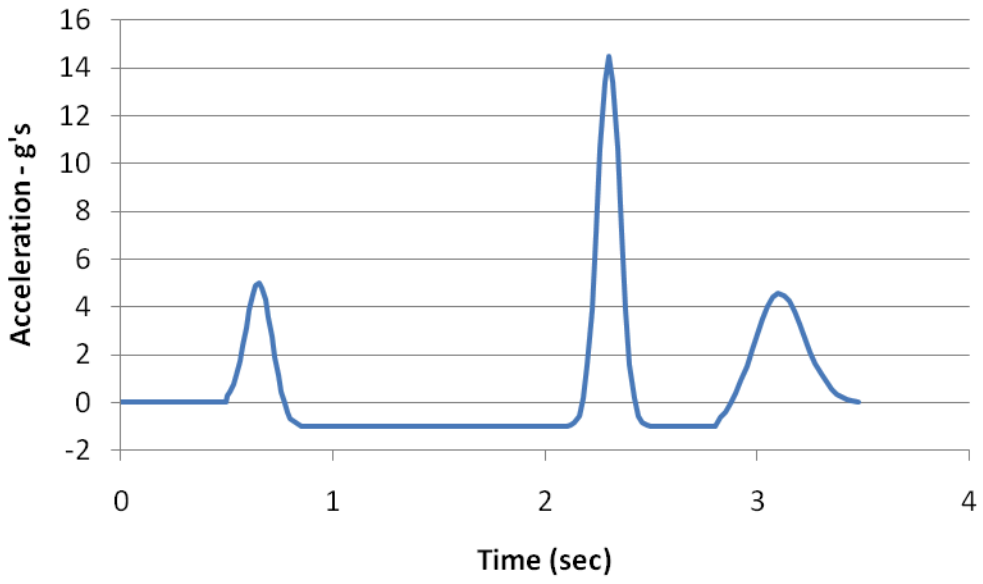

Figure A-1. Typical time history of the acceleration at surface ground zero for an underground explosion, where there is spalling of the surface. The first peak is due to the initial shock from the explosion. The period at -1 g is where the surface is in free fall back down. The large peak occurs when the surface layer slams down against underlying material. The third peak is due to a reflected compression wave in the surface layer.

A.2 Peak acceleration near GSZ

Scaling relations have been developed to estimate the peak surface acceleration a (in g's) near GSZ taking into account yield Y in kt, depth of burial (DOB) D in meters, surface distance r from SGZ in meters, and rock type [Schoutens, 1979]. The generic scaling relation for peak acceleration is given by [Schoutens, 1979, equation IV-2.3]:

$$a = Y^{1/3} * A * (R/Y^{1/3})^{-p},$$

where A and p are constants depending on the rock type, and R is the slant range from the explosion to the surface point given by

$$R = (D^2 + r^2)^{1/2}.$$

The acceleration can be much higher near GSZ for hard rock such as granite compared to other materials, such as alluvium. Some empirical formulas for peak vertical acceleration from tests at the NTS are [derived from Figures IV-2.32, IV-2.33, and IV-2.34 in Schoutens, 1979]:

$a^* Y^{1/3} = 2.37e7 * (R/Y^{1/3})^{-3.20}$	(1.04 g's)	NTS Alluvium, type 1
$a^* Y^{1/3} = 2.52e7 * (R/Y^{1/3})^{-3.05}$	(2.46 g's)	NTS Alluvium, type 2
$a^* Y^{1/3} = 1.69e6 * (R/Y^{1/3})^{-2.34}$	(6.9 g's)	Tuff-Rainier Mesa

$a^* Y^{1/3} = 1.08e9 * (R/Y^{1/3})^{-3.23}$ (40 g's) Tuff-Antler Mesa
$a^* Y^{1/3} = 6.58e8 * (R/Y^{1/3})^{-3.04}$ (67.4 g's) Granite and salt

where a is in g's, Y is in kt, and R is in meters. The acceleration shown in parentheses is the surface acceleration at SGZ for the baseline scenario (1 kt yield at 200 m DOB). Note the peak acceleration may vary by a factor of a few for nominally similar materials, and that there is about a factor of 65 difference in acceleration over the range of measured materials.

A.3 Spatial dependence of surface acceleration

The purpose of this section is to estimate the approximate spatial extent for which accelerations close to the peak acceleration will be present on the surface. Various authors have come to significantly different conclusions about how the surface acceleration drops off with range from SGZ, but those differences do not impact the conclusion that the acceleration on the surface is within a factor of two of the peak acceleration out to a radius of approximately 0.7 to 2.0*DOB. As can be seen in section A.5, surface acceleration is highly dependent on local geology and may show spatial variations not indicated by these simple formulae.

From Schoutens [Schoutens, 1979] (see exponents in Section A.2 equations), the acceleration drops off as approximately the inverse cube of the slant range from the explosion to the surface point. One would naively expect the acceleration to vary as the inverse square of the slant range because the compressive force of the explosion is distributed over the surface of a sphere with the slant range radius. However, at the surface near SGZ, the compression wave is normal to the surface and reflected back into the ground, which roughly doubles the surface acceleration. Farther from SGZ, the compression wave becomes tangential to the surface, so the reflected compression wave and surface acceleration diminishes with surface angle as well as slant range. This means the acceleration should drop off faster than an inverse square relation, which is consistent with the measured inverse cube relation. For an inverse cube relation, the surface acceleration is within a factor of two of the peak acceleration out to a radius of 0.77*DOB.

In contrast, MacQueen [MacQueen, 1982] finds that the surface acceleration drops off less quickly than the naively expected inverse square relation. In MacQueen, 1982, Figure 4 shows the first peak surface acceleration to drop by about 10% between SGZ and a surface range of 1250 m for DOB=640 m, and Figure 5 shows about a 20% drop in the acceleration of the slapdown peak between SGZ and a range of 1250 m for the same event ("Event A"). Figure 11 shows the first peak acceleration to have dropped from 63 m/s^2 at SGZ to 57 m/s^2 at a surface range of 760 m (compared to DOB=701 m). This drop off is even slower than a simple inverse square relation with slant range. Since the data here were only referred to as "Event A" and "Event B", it is not possible to check whether the two references are using the same data. For these two events, the surface acceleration did not drop to half its SGZ value until a radius of 1.5 to 2.0*DOB.

The difference in spatial scaling between these two references may be due to the use of vertical accelerations in Schoutens, 1979, and total acceleration in MacQueen, 1982. Certainly the exclusion of horizontal acceleration in Schoutens will result in a more rapid drop off of acceleration with surface range than would otherwise be the case. The difference between the two spatial scaling relations is not significant for the purposes here, and is much smaller than the variation in the amplitude of surface acceleration due to geological materials.

A.4 Caveats on use of surface acceleration to estimate surface disruption

We assume here that plant stress and disruption of surface material are dependent on peak acceleration, regardless of direction. Surface velocity and surface displacement were assumed to be less important since those motions by themselves do not necessarily cause disruption effects. However, one could make the case that the amount of acceleration and the ***time*** that acceleration was present would be a better figure of merit for the amount of disruption, because the impulse (change in momentum) given to surface materials will be proportional to the acceleration and the amount of time the acceleration is present. Another way to look at it is that what matters is the energy transferred to the surface materials. Since the kinetic energy equals $\frac{1}{2}*m*v^2$, both of these perspectives suggest velocity (nominally equals acceleration x time) as an alternate predictor of surface disruption. Since the existing data on plant stress were measured against surface acceleration, we have chosen to use acceleration here. The reader is cautioned that future experiments might also measure surface velocity as a metric for surface disruption. The literature, including references herein, typically has velocity data at least as complete and accurate as the acceleration data.

The reader should also note that references do not always distinguish the initial acceleration peak (from the initial compression wave reaching the surface) from the peak acceleration (typically due to slapdown in the spall zone). Also, vertical acceleration is often the only reported quantity, whereas total acceleration is probably the important quantity here. Since the peak acceleration is expected at SGZ, and the acceleration should be vertical there, the estimates of peak acceleration at SGZ should be unaffected by this detail. However, Schoutens, 1979, did not report values for horizontal accelerations. With increasing range from SGZ, the horizontal component of the acceleration will increase until the reduction with range overcomes the increase with slant angle. This means that the total surface acceleration will drop less quickly with surface range than the inverse cube relation derived from the data in that reference. For an inverse square relation for total acceleration, the vertical component would be proportional to D/R, so the vertical acceleration as a function of slant range would be proportional to $1/R^3$, as observed. Taking into account both the vertical (incoming and reflected) and horizontal components, the surface acceleration is given by

$a = a_0 * (R/D)^{-3} * 0.5 * (3D^2 + R^2)^{1/2}$,

where a_0 is the surface acceleration at SGZ. Some of the data in Schoutens, 1979, did go out to longer ranges, where they started to show a transition to a less rapid drop off of acceleration with slant range. Using this more general formula, the surface acceleration drops to half its SGZ value at a surface range of 0.82*DOB.

Figure A-2 shows the total, vertical and horizontal components of the scaled acceleration when the vertical acceleration is doubled by the reflected compression wave. For the region near SGZ, the vertical component is dominant. One could make an argument that horizontal accelerations would have a more significant impact on plant stress and surface disruption since typical horizontal stresses (e.g., from wind) are typically much less than the vertical stress of gravity. Figure A-2 also shows an effective acceleration curve for when the horizontal acceleration has 4x the disruptive impact of a vertical acceleration. While that pushes the half-acceleration point out to 1.6*DOB (versus 0.8*DOB for the nominal model), the main qualitative effect is a broadening of the spatial region where disruption effects will be very similar to those around SGZ. This means there may be a physical mechanism of surface disruption that would generate a much more uniform amount of disruption near SGZ than would be the case if surface disruption was simply correlated with total acceleration.

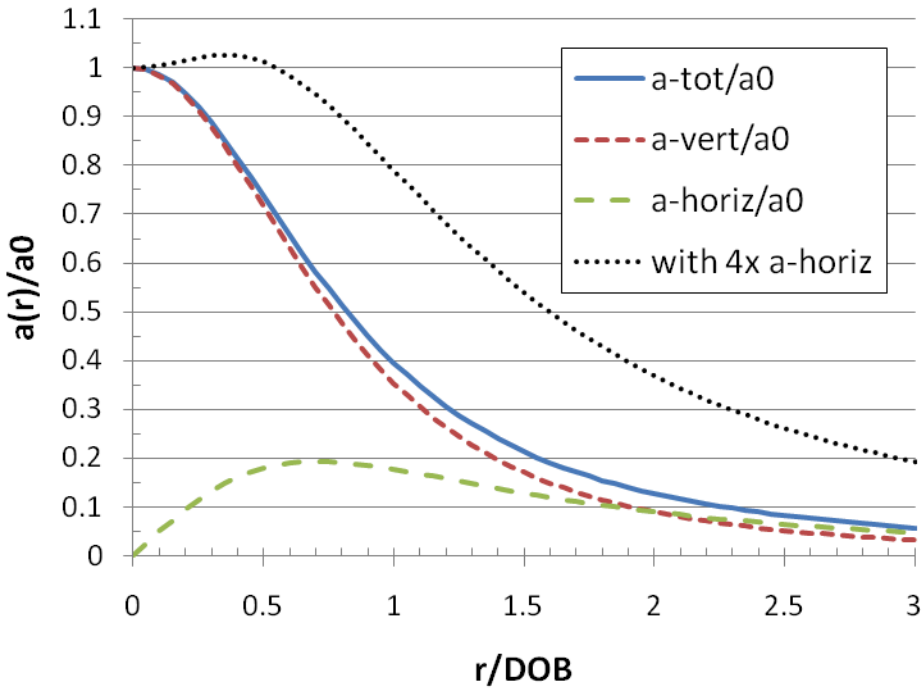

Figure A-2. Comparison of vertical (red medium dash) and horizontal (green large dash) components of the surface acceleration to the total acceleration (blue solid line), and to an effective total acceleration where the horizontal component of the acceleration causes 4x the surface disruption of the vertical component (black fine dash).

A.5 Comparison to NPE data

The magnitude of the surface acceleration was measured during the non-proliferation experiment (NPE) and varied from a peak of 2.7 g, to more than 0.2 g at ranges out to 2 km from SGZ. Table A-1 gives the three components of the total surface acceleration for six ground stations. The Table has been arranged so the entries are listed in order of increasing range from SGZ, and the accelerations are therefore expected to decrease monotonically down the Table. However, there is considerable variation in the accelerations, most likely due to the fact that the local geology is not homogeneous. For these ranges, the DOB is about half the surface range, so one expects the radial acceleration and the vertical acceleration to be comparable since the vertical acceleration is doubled by reflection from the surface. The Table shows that the radial (R) and vertical (Z) accelerations are in fact close to each other. Also, in a homogeneous medium, one would expect the transverse acceleration to be zero. Here, the transverse acceleration is about half the radial or vertical component, which is consistent with the local geology being inhomogeneous, as had been concluded from the non-monotonic behavior of the total acceleration as a function of range.

Table A-1. Maximum Accelerations from NPE (adapted from Johnson, 1994, Table 2). Values shown are from 6 accelerometer stations at a variety of azimuths and range from SGZ. The DOB is added in quadrature to get the range from the event. Max R, T and Z refer to the maximum acceleration in the radial, transverse and vertical directions respectively.

Station	Azimuth Deg	SGZ Range m	GZ Range m	Max R g	Max T g	Max Z g
UCB 140	270	599	709	1.34	0.72	1.47
UCB 160	259	616	724	0.63	0.27	0.73
UCB 120	279	656	759	0.81	0.47	0.67
UCB 180	249	668	769	0.96	0.62	1.07
UCB 100	285	747	841	0.43	0.35	0.66
UCB 200	242	762	853	0.83	0.36	0.61

Figure A-3 shows a different set of acceleration data acquired during the NPE. Here, peak accelerations are shown relative to the location of the NPE SGZ, and in the context of the NPE location on Rainier Mesa at the Nevada Test Site. It is interesting to note that the peak accelerations greater than 1.0 g are sometimes found farther from SGZ than regions of intermediate acceleration (0.2 to 1.0 g). The important point from this data is that the complex geology for the NPE means that the simple models developed here for acceleration as a function of range should only be used as a starting point for the spatial distribution of acceleration-induced observables, and that local geology can induce regions of high surface acceleration at relatively long ranges from SGZ.

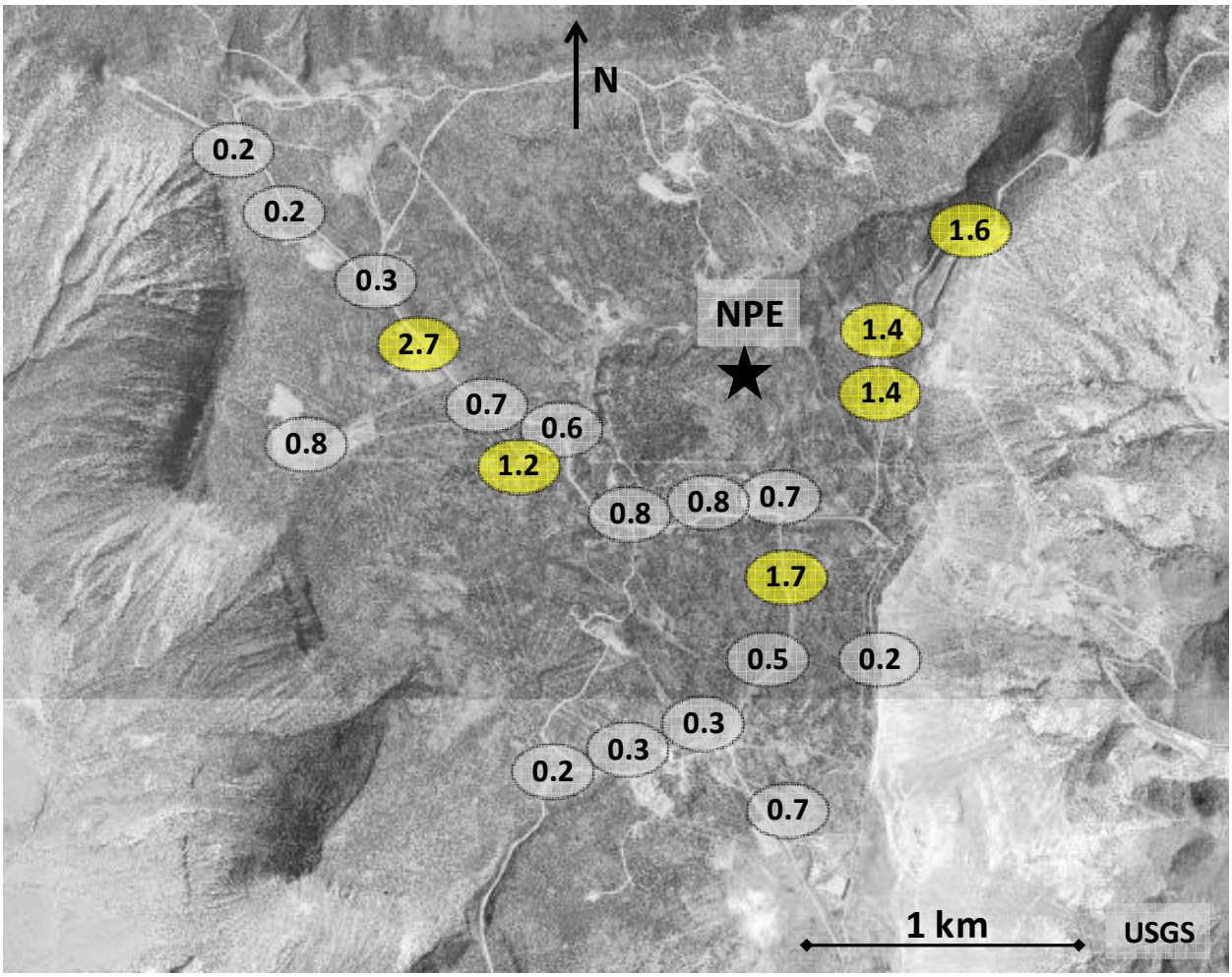

Figure A-3. Measured maximum surface accelerations for the NPE, in g's, superimposed on imagery of the NPE location at Rainier Mesa from the U.S. Geological Survery. Note that accelerations greater than 1 g (highlighted in yellow) are often sandwiched between regions of lower acceleration. (Adapted from Pickles, 1995, Figure 5.)

ACKNOWLEDGEMENTS

The editor would like to acknowledge the many valuable discussions, careful review of the manuscript, and comments and suggestions provided by Paul Rockett, Milton Smith, and Michael Zelinski of Lawrence Livermore National Laboratory.

REFERENCES

Adushkin, V. V. and Spivak, A. A, "Geologic characterization and mechanics of underground nuclear explosions", Defense Nuclear Agency Technical Report, 1994 (Contract No. DNA 001-93-C-0026).

Adushkin, V. V. and Leith, W., "Containment of Soviet Underground Nuclear Events", USGS Open File Report 01-312, Sept 2001.

Anderson, J. G., and Brune, J. N., "Extreme Ground Motion Studies", Nevada System of Higher Education Document Number SIP-UNR-049, July 2006.

Bernreuter, D. L., Jackson, E. C., and Miller, A. B., "Control of the Dynamic Environment Produced by Underground Nuclear Explosives," LLNL publication UCRL-72122, December 1969.

Brand, D., "Considerations for Selecting Initial Overflight Equipment," OSI Workshop-2, February 1998.

Busygin, V. P., Nizamov, A. G., Khoklov, U. P., and Shchipletsov, M. V., "Heat-radiation Displays in an Epicentral Zone of an Underground Nuclear Explosion," OSI Workshop 6, June 2000.

Button, P., "Application of Geochemical Techniques to CTBT On-Site Inspection," OSI Workshop-2, February 1998.

Button, P. and Hall, G, "Geochemical Signatures Observed over Horizontally Emplaced Underground Nuclear Tests," OSI Workshop-3, November 1998.

Carter, G. A., "Responses of Leaf Spectral Reflectance to Plant Stress," American Journal of Botany 80(3), 239-234, 1993.

Carter, G. A., "Ratio of Reflectance in Plant Stress," International Journal of Remote Sensing 15(3), 697–703, 1994.

Clark, R. N. 1999, Manual of Remote Sensing, ed. A. Rencz (J.Wiley and Sons, New-York).

Davies, A., "On-Site Inspections – Equipment to be Used in Initial and Later Overflights," OSI Workshop-2, February 1998.

Dubasov, Y. V., "Basic Requirements to Instruments and Equipment used to Conduct Radiation Measurements On-Site Inspection," OSI Workshop-2, February 1998.

Eisler, J. D. and Chilton, F., "Spalling of the Earth's Surface by Underground Nuclear Explosions," Journal of Geophysical Research, Vol 69, No. 24, p5285, 1964.

Hall, G. E. M., Vaive, J. E., and Button, P., "Detection of past underground nuclear events by geochemical signatures in soils," Journal of Geochemical Exploration, 1529 (1997).

Hawkins, W. and Wohletz, K., "Visual Inspection for CTBT Verification," LANL publication LAMS-13244-MS, November 1996 (presented at OSI Workshop-1, July/August 1997).

Hawkins, W., "Ground-Based Visual Observation Activities and Data Management: Equipment for the Initial Survey of the Inspection Area," OSI Workshop-2, February 1998.

Henderson, J. R., Smith, M. O., and Zelinksi, M. E., "Overhead Detection of Underground Nuclear Explosions by Multi-Spectral and Infrared Imaging," LLNL publication LLNL-TR-459432, September 2010.

Gough, R., "US Table Top Exercise", OSI Workshop-3, November 1998.

Johnson, G. W., Higgins, G. H., and Violet, C. E., "Underground Nuclear Explosions," Journal of Geophysical Research, Vol 64, No. 10, October 1959.

Johnson, L. R., "Recording Experiment on Rainier Mesa in Conjunction with a Reflection Survey", Proceedings of the Symposium on the Non-Proliferation Experiment: Results and Implications for Test Ban Treaties, 1994, Department of Energy CONF-9404100.

Kamm, J. R., and Bos, R. J., "Comparison of chemical and nuclear explosions: Numerical simulations of the Non-Proliferation Experiment", LANL Report LA-12942-MS, June 1995.

MacQueen, D. H., "An Analytic Model for Surface Ground Motion with Spall Induced by Underground Nuclear Tests," LLNL Report UCRL-53266, April 1982.

Marshall, P. D., "Basic Presentation of the Subject Leader," OSI Workshop-1, August 1997.

Olsen, C. W., "Site Selection and Containment Evaluation for LLNL Nuclear Events," LLNL publication UCRL-JC-113334, p 16, 1993.

Patton, H. J., "Investigations of the Low Frequency Seismic Waves Recorded at Near-Regional Distances from the Non-Proliferation Experiment," Proceedings of the Symposium on the Non-

Proliferation Experiment (NPE): Results and Implications for Test Ban Treaties, April 1994, DOE, CONF-9404100.

Pickles, W. L., "Observations of Temporary Plant Stress Induced by the Surface Shock of a 1 kt Underground Chemical Explosion," LLNL publication UCRL-ID-122557, December 1995.

Pickles, W. L. and Carter, G. A., "Detecting Plant Metabolic Responses Induced by Ground Shock Using Hyperspectral Remote Sensing and Physiological Contact Measurements," LLNL publication UCRL-ID-127061, December 1996.

Pickles, W. L., personal communication, August 2010.

Proceedings of the Symposium on the Non-Proliferation Experiment (NPE): Results and Implications for Test Ban Treaties, April 1994, DOE, CONF-9404100.

Rhoads, W. A., "Ground Motion Effects of Underground Nuclear Testing on Perennial Vegetation at Nevada Test Site," EGG-1183-2317, 1976.

Rockett, Paul, "Multi-spectral Imaging in a CTBT OSI," On-Site Inspection Workshop-5, November 1999.

Russian Federation, "Working Paper 1," OSI Workshop-1, August 1997.

Sakharov, Y. A, "Initial Survey of Inspection Area: Requirements to Equipment at Limitation of Operations", OSI Workshop-2, February 1998.

Schoutens, J. E*., Nuclear Geoplosics Sourcebook. Volume IV. Part I. Empirical Analysis of Ground Motion from Above and Underground Explosions*. Defense Nuclear Agency publication DNA 6501H-4-1, 1979.

U.S. Congress, Office of Technology Assessment, "The Containment of Underground Nuclear Explosions", OTA-ISC-414 (Washington, DC: U.S. Government Printing Office, October 1989).

Wang, L., Qu, J. J., Xiong, X., and Hao, X., "Analysis of seven-year moderate resolution imaging spectroradiometer vegetation water indices for drought and fire activity assessment over Georgia of the United States," Journal of Applied Remote Sensing, Vol. 3, 033555, (8 October 2009).

Zucca, J. J., Carrigan, C., Goldstein, P., Jarpe, S. P., Sweeney, J., Pickles, W. L., and Wright, B., "Signatures of Testing: On-Site Inspection Technologies", LLNL publication UCRL-JC-119213, January 1995.

Zucca, J. J., Rapporteur, "Report of the On-Site Inspection Workshop," August 1997, p 11.

FIGURE CREDITS

Figure 3-1. Image from http://www.rsacl.co.uk/rs.html.

Figure 6.1-1. Paul Rockett, "Multi-spectral Imaging in a CTBT OSI," On-Site Inspection Workshop-5, November 1999, p 11.

Figure 6.1-2. Left image derived from Landsat data. Right image from Google Earth.

Figure 6.2-1. Adapted from Clark, R. N. 1999, Manual of Remote Sensing, ed. A. Rencz (J.Wiley and Sons, New-York).

Figure A-1. Original material by author.

Figure A-2. Original material by author.

Figure A-3. Imagery courtesy of U.S. Geological Survey. Surface acceleration data from reference Pickles, 1995, figure 5.

ACRONYM LIST

CONOPS	Concept of Operations
CTBT	Comprehensive Nuclear Test Ban Treaty
DOB	Depth of burial
DSP	Defense Support Program
IA	Inspection Area
IMS	International Monitoring System
ISP	Inspected State Party
GPS	Global Positioning Satellite
GZ	Ground Zero
LANL	Los Alamos National Laboratory
LLNL	Lawrence Livermore National Laboratory
LOS	Line of sight
LWIR	Long-Wave Infra Red
MSIR	Multi-Spectral and Infra Red imaging
OSI	On-Site Inspection
NPE	Non-Proliferation Experiment
NTS	Nevada Test Site
PTS	Provisional Technical Secretariat
SGZ	Surface Ground Zero
UAV	Unmanned Aerial Vehicle
UNE	Underground Nuclear Explosion